ISBN: 978-93-94570-41-2

5. Optimization of Ejector Design Using CFD Analysis

Dr. D. Raja Joseph

Associate Professor,
School of Aeronautical Sciences,
Hindustan Institute of Technology and Science.

Dr. R. Christu Paul

Professor,
Department of Automobile Engineering,
Hindustan Institute of Technology and Science.

Abstract:

The satellite launch vehicle, GSLV has a cryogenic upper stage, which uses the cryogenic engine. In order to test and qualify the upper stage engine, used in a high-altitude Test Facility is used. The HAT facility is configured with a vacuum chamber, a second throat diffuser, a gas cooler, and an ejector and the diffuser system. Each subsystem has to be analyzed numerically and optimized for its better performance. This report deals with the Ejector system. In the first step, the basic dimensions of the ejector are derived from the one-dimensional gas dynamic equation. This report describes the performance of Ejector (designed by ID), the need for optimization, optimization of the Ejector system using CFD. A 2 – dimensional axis-symmetric geometry with nozzle and mixer system is considered for the analysis. A two – dimensional structured mesh, standard k-ε modeling for turbulence and species transport (not reacting) equations for species transport is considered for the analysis. The effect of varying the Nozzle exit diameter was studied to optimize the ejector for both no-load and full load conditions using CFD fluent software.

5.1 Introduction:

Leading countries in the world like the USA, USSR, France, China, India, etc. are involved in space research and developing their nations in various fields like defense, telecommunication, weather forecasting, etc. Nowadays space technology has become a part of the everyday life of millions of people.

A good example is the mutest images we see on the television screen. A communication satellite has revolutionized global communication which holds great promise for the near future. Satellite observations are increasingly important for accurate and timely weather forecasting. Such developments will exert even greater influences in our living conditions and quality of life. A satellite is a payload carried by the launch vehicle and injected into the desired orbit. Generally, there are six types of satellites. They are a military satellite, weather satellite, communication satellite, Navigation satellite, space research satellite, and bio satellite. A satellite is generally launched towards the east so as to take advantage of the earth's eastward rotation. The satellite moving from west to east in a circular orbit of about 36000 km above the equator takes 24 hrs.

5.2 Related Works:

E.J.; DeHart, J.H studied combination of computer analysis and scale model testing was utilized to develop a nozzle that would increase the performance of thrust augmentation ejectors, Scale model tests were conducted on various multi-lobed and vortex generating nozzles. Predicted jet characteristics were obtained by calculating a finite difference solution of Reynolds equations for the three-dimensional flow field. A two-equation turbulence kinetic energy model was used for closure. It is demonstrated that the thrust augmentation of the XFV-12A ejector can be increased from 1.45 to 1.4 by the addition of lobes to the baseline nozzle, and a corresponding increase of throat width.

The report documents the WIND k-epsilon model validation results for a two-dimensional ejector nozzle flow by Gilbert, G.B., and Hill, P.G.Comparisons are made between the NPARC and WIND k-epsilon model implementations and with the WIND SST model results. In addition, the effects of the Sarkar compressibility correction and the variable C mu option on the stability and convergence of the WIND k-epsilon model are discussed by Gilbert, G.B., and Hill, P.G.The focus of this investigation was the turbulent flow through a two-dimensional ejector nozzle which was tested by Gilbert and Hill (1973).

This flow features the turbulent mixing between the primary jet entrained secondary air as well as the interaction with the wall boundary layers. The rectangular mixing section is formed by the symmetrically contoured upper and lower walls and the two flat sidewalls.

The widths of both the primary nozzle discharge slot and the mixing section were 8.00 inches. Suction slots were placed in the corners of the mixing section to prevent flow separation. The experimental data to be used for comparison purposes consists of velocity and temperature measurements at several axial locations. The inflow conditions used in the numerical computations correspond to those of run 9 in the report by Gilbert and Hill (1973).

V. M. Puzyrev and R. K. Tagirov proposed method for calculating the two-dimensional non-viscous flows in ejector nozzles of arbitrary shape, for two operating cycles: the subsonic flow cycle of a secondary stream and a cycle when the secondary stream attains critical velocity i.e.; it is cut off, the possibility is allowed for the appearance of a direct compression shock in the supersonic part of the secondary stream

Emilia Wagnerova, Ivan Imri s developed the continuous production of copper dried concentrate and fluxes were injected through the top-blowing lance into the molten bath. The properties of the equipment designed were determined by both classical measurements of the airflow parameters through an ejector with an annular supersonic nozzle that was confirmed by the sheer and the shade methods of flow visualization.

Vaclav Dvorak, Pavel Safarik deals with an experimental, theoretical and numerical study of the interaction of supersonic flows on the trailing edge of a primary flow nozzle of an ejector. The mechanism of mutual deflection of supersonic flows is explained. The influences of backpressure and stagnation pressure ratio of both flows on the interaction are presented. Recommendations for the design and for the operation of supersonic ejectors are formulated.

The satellite launch vehicle consists of different stages that have a cryogenic upper stage, which uses the cryogenic engine. In order to test and qualify the upper stage engine, high altitude test facility is required. The HAT facility is configured with a vacuum chamber, a second throat diffuser, a gas cooler, and an ejector and the diffuser system.

Each subsystem has to be analyzed numerically and optimized for its better performance. This report deals with the Ejector system. In the first step, the basic dimensions of the ejector are derived from the one-dimensional gas dynamic equation.

This report describes the better performance of Ejector, need for optimization of the ejector system using CFD. A 2d axis-symmetric geometry with nozzle and mixer system is considered for the analysis. A 2d structured mesh standard k- ε modeling for turbulence and species transport is considered for the analysis.

Based on the above cases, the optimum configuration of the ejector system with the nozzle A.R of 4.6, the distance between the nozzle exit and the mixer throat of 925 mm.

The GN2 supply pressure of 25 bars has arrived through detailed CFD analysis which yields the better performance of No-load suction Pr. Of 22.9 m bar and the full load suction pressure of 784.85m bar. It is exactly matching with the one-dimensional gas dynamic equation value as well as the system requirement of cryo-rocket engine HAT facility.

5.3 Materials and Methods:

5.3.1 Computational domain and grids:

A 2 – dimensional axisymmetric geometry with nozzle and mixer system is considered for the numerical analysis.

The geometry is done in the CAD system and it is imported in Gambit. Structured mesh has been used throughout the analysis and the total number of nodes was 68734.

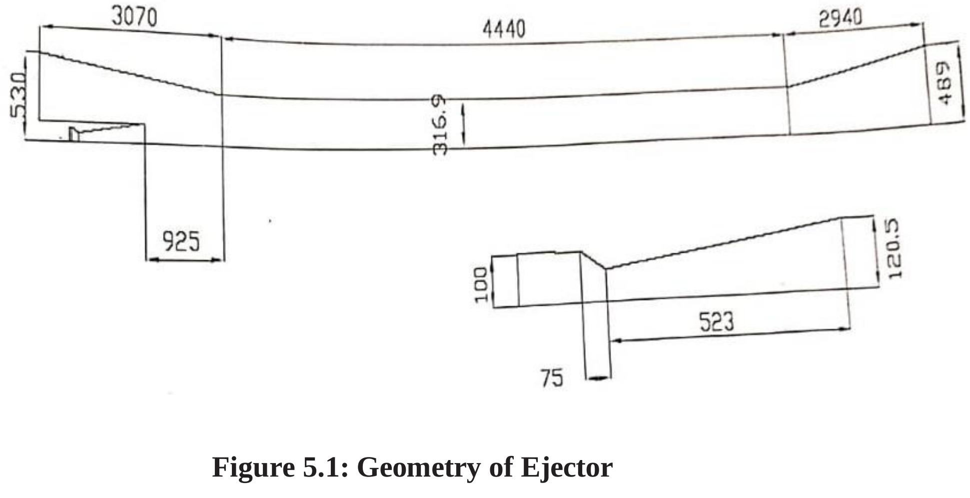

Figure 5.1: Geometry of Ejector

5.3.2 Numerical methods:

Gambit is a preprocessor that is used for geometry preparation and grid generation. Using Gambit 2-D and 3-D geometries can be drawn. Realistic geometries are too complicated to be generated in Gambit. So, the design is done in the CAD system and it is imported into it. Gambit is based on ACIS geometrical system which is the most widely used 3-D modeling technology. It can also import STEP, IGES STL files.

The geometry or topology of Gambit is Vertex, Edge, Face, Volume.

5.3.3 Governing equations:

The governing flow equation based on the physical principle that energy is conserved is known as the "Energy Equation".

$$\frac{\partial \rho E}{\partial t} - div(\rho E V) = \frac{\partial (u\tau_{xx})}{\partial x} + \frac{\partial (u\tau_{yx})}{\partial y} + \frac{\partial (u\tau_{zx})}{\partial z} + \frac{\partial (v\tau_{xy})}{\partial x} + \frac{\partial (v\tau_{yy})}{\partial y} + \frac{\partial (v\tau_{zy})}{\partial z} + \frac{\partial (w\tau_{xz})}{\partial x} + \frac{\partial (w\tau_{yz})}{\partial y} + \frac{\partial (w\tau_{zz})}{\partial z} + \frac{\partial}{\partial x}\left[k\frac{\partial T}{\partial x}\right] + \frac{\partial}{\partial y}\left[k\frac{\partial T}{\partial y}\right] + \frac{\partial}{\partial z}\left[k\frac{\partial T}{\partial z}\right] + S_g$$

In the above equation, a divergence term appears on the left-hand side. These terms involve the divergence of the flux of some physical quantity: ρV, ρuV, $\rho vV, \rho wV \rho EV$.

These flux terms are solved during a CFD analysis and the primitive variables can be calculated from them.

The k-ϵ model is the most widely used and validated turbulence model. It has achieved notable success in calculating the wide variety of thin shear layer and recirculating flows without the need for case-by-case adjustment of the model constants.

The model performs particularly well in confined flows where Reynolds shear stress is most important. Some reasons to select this model for the present work are

- Simplest turbulence model for which only initial and boundary conditions need to be supplied.
- Excellent performance for many industrial relevant flows.
- Well established, most widely validated turbulence model

The transport equations for this model are as follows

Turbulent energy (k)

$$\frac{\partial}{\partial t}(\rho)+\frac{\partial}{\partial x_i}\left[\rho u_j k-(\mu+\frac{\mu_t}{\sigma_k}\mu_{t)}\frac{\partial k}{\partial x_j}\right]$$
$$=\mu_t(P+P_B)-\rho\varepsilon-\frac{2}{3}\left(\mu\frac{\partial u_i}{\partial x_i}+\rho k\right)\frac{\partial u_i}{\partial x_i}+\mu_t P_{NL}$$

Where

$$\mathrm{P}=2S_{ij}\frac{\partial u_i}{\partial x_j} \qquad P_B=-\frac{g_1}{\sigma_{h,t}}\frac{1}{\rho}\frac{\partial P}{\partial x_i}$$

$$P_{NL}=-\frac{\rho}{\mu_t}\mu_i'\mu_j'\frac{\partial \mu_i}{\partial x_j}-\left[P-\frac{2}{3}\left(\frac{\partial \mu_i}{\partial x_i}+\frac{\rho k}{\mu_t}\right)\frac{\partial \mu_i}{\partial x_i}\right]$$

$P_{NL}=0$ for nonlinear models and σ_k is an empirical coefficient.

The first term on the right-hand side of the turbulent energy equation represents turbulent generation by shear and normal stresses and buoyancy forces, the second viscous dissipation and the third amplification or attenuation due to compressibility effects.

The last term accounts for non-linear contributions. Turbulence dissipation rate (ε)

$$\frac{\partial}{\partial t}(\rho\varepsilon)+\frac{\partial}{\partial x_j}\left[\rho u_j\varepsilon-(\mu+\frac{\mu_t}{\sigma_\varepsilon}\mu_{t)}\frac{\partial \varepsilon}{\partial x_j}\right]$$
$$=C_{\varepsilon 1}\frac{\varepsilon}{k}\left[\mu_t P-\rho\varepsilon-\frac{2}{3}\left(\mu\frac{\partial u_i}{\partial x_i}+\rho k\right)\frac{\partial u_i}{\partial x_i}\right]+C_{\varepsilon 3}\frac{\varepsilon}{k}\mu_t P_B-C_{\varepsilon 2}\rho\frac{\varepsilon^2}{k}$$
$$+C_{\varepsilon 4}\rho\varepsilon\frac{\partial u_i}{\partial x_i}+C_{\varepsilon 1}\frac{\varepsilon}{k}\mu_t P_{NL}$$

Where $\sigma_{\varepsilon,}C_{\varepsilon 1},C_{\varepsilon 2,}C_{\varepsilon 3}$ and $C_{\varepsilon 4}$ are the empirical coefficients whose values are given in the table.

The right-hand side terms represent the analogous effects to those described above for the k equation.

The turbulent viscosity $\mu_t = f_\mu c_\mu \rho \, {k^2}/{\varepsilon}$ with f_μ set equal to unity.

C_μ	0.09
σ_k	1.0
σ_ε	1.22
$C_{\varepsilon 1}$	1.44
$C_{\varepsilon 2}$	1.92
$C_{\varepsilon 3}$	1.44
$C_{\varepsilon 4}$	-0.33
k	0.42

5.3.4 Boundary Conditions:

The inlet pressure and temperature were 25bar and 250 k and outlet pressure as 1 bar and 300 k.

Case 1

Effect of Area ratio of GN2 supply Nozzle on the Ejector system:

The effect of area ratio on ejector no load & full load variations are given in table 5.1 & 5.2.

Table 5.1: Results of No-load Analysis

Area Ratio	Operating Pressure (bar)	No-load Pressure
4.4	25	34.78

Area Ratio	Operating Pressure (bar)	No-load Pressure
4.6	25	22.9
4.8	25	175.07

Table 5.2: Results of Full load analysis

Area Ratio	Operating Pressure (bar)	Full load Pressure (m bar)
4.4	25	916.04
4.6	25	784.75
4.8	25	911.85

Effect of the area ratio of GN2nozzle:

From the above results, the observations are as followed.

In this case, three area ratios 4.4,4.6,4.8 have been considered for the ejector nozzle. The GN2 supply pressure is kept constant (pressure=25 bar). The spacing of the ejector Nozzle exit from the mixer throat is kept constant (d=925 mm).

The No-load suction pressure obtained for the ejector is 34.78m bar, three cases as shown in table 5.1. It is found that the suction pressure at no load and full load for area ratio 4.6 is the lowest and it is matching with the one-dimensional value as per the design document of Cryo-rocket engine HAT facility.

Based on the above result the optional area of 4.6 is arrived for the desired no load and full load pressure. The tangential shear mixing of passive and active fluid is achieved as the area ratio 4.6. The Variations of Static Pressure static temperature, Mach Number, flow velocity for No-load as well as Full load conditions with area ratio 4.6 are given in figures.

Effect of Ejector spacing for constant area ratio on the ejector system:

The effect of Ejector spacing for constant area ratio no load & full load variations are given in table 5.3 & 5.4.

Table 5.3: Results of No-load Analysis

Length (mm)	Operating Pressure (bar)	No-load Pressure (m bar)
850	25	32.47
925	25	22.9
1000	25	37.23

Table 5.4: Results of Full load Analysis

Length (mm)	Operating Pressure (bar)	Full load Pressure (m bar)
850	25	915.19
925	25	784.75
1000	25	909.7

Effect of GN2 supply nozzle exit plane location from the mixer throat:

From the above results, the observations are as followed.

The spacing of ejector Nozzle exit from the mixer throat is varying 850 mm,925 mm and 1000 mm have been considered for the ejector Nozzle for constant area ratio 4.6. The GN2 Supply pressure is kept constant (pressure = 25 bar).

The No-Load suction pressure obtained for the ejector is 32.47 m bar,22.9m bar,37.23m bar for the three cases as shown in table 5.3. It is found that the suction pressure at No load and full load for the distance of 925 mm and it is matching with the one-dimensional value as per the design document of the Cryo-rocket engine HAT facility.

In general, no-load pressure parallel the small spacing from mixture throat at the minimum and full load pressure parallel be higher. Based on the above result the spacing of 925 mm is suitable for the no-load and full load pressure requirement.

The variations of Static Pressure, Static Temperature, Mach Number, Flow Velocity for No-load as well as Full load conditions with area ratio 4.6 are given in figures.

Case 3:

Effect of GN2 supply flow rate:

Table 5.5: Results of No-load Analysis:

Operating Pressure (bar)	GN2 Flow rate (Kg/s)	No-load Pressure
20	48.29	279.35
25	60.18	22.9
30	72.44	27.89

Table 5.6: Results of Full load analysis:

Operating Pressure (bar)	GN2 Flow rate (Kg/s)	Full load Pressure (m bar)
20	48.29	902.39
25	60.18	784.75
30	72.44	919.01

Effect of GN2 supply flow rate:

From the above results, the observations are as followed. In this case, three operating pressure 20 bar, 25 bar, and 30 bar have been considered for the ejector Nozzle area ratio is 4.6 and the Nozzle exit from the mixer throat is 925 mm. The GN2 flow rate obtained for the ejector is 48.29,60.18,72.44 for the three cases as shown in table 5.5. It is found that the suction pressure at No load and Full Load for pressure 25 bar is the lowest and it is matching with the one-dimensional value as per the design document of Cryo-rocket engine HAT facility.

The ejector mixer throat is designed for the chocking condition of the desired flow rate. Based on the above, the optimum of the GN2 supply rate of 60 kg/s is best suitable for the desired no load and full load condition. The variations of Static Pressure, Static Temperature, Mach Number, Flow Velocity for No-load as well as Full load conditions with area ratio 4.6 are given in figures.

5.4 Results and Discussion:

PC=20bar; MGN2=48kg/s

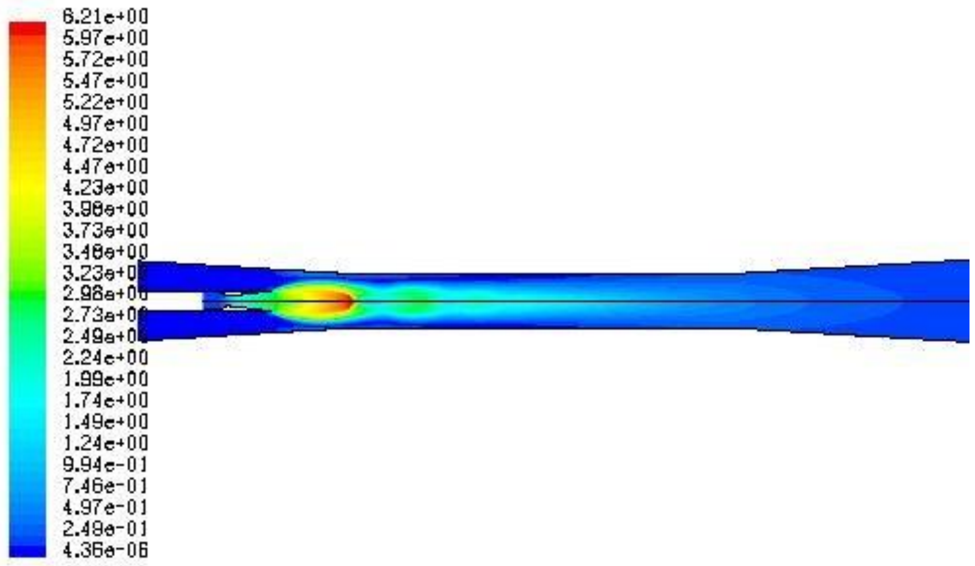

Contours of Mach Number

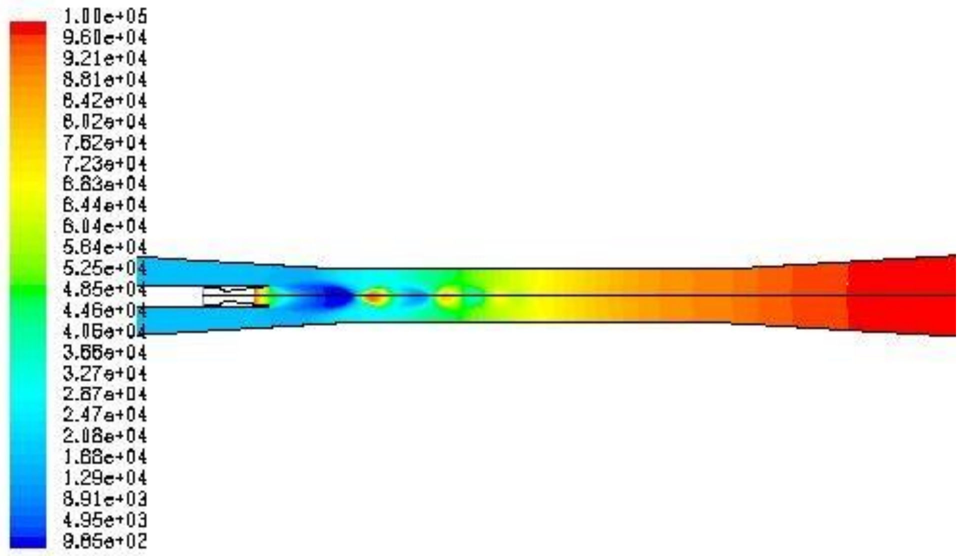

Contours of Static Pressure (pascal)

PC=22.5bar;MGN2=54kg/s

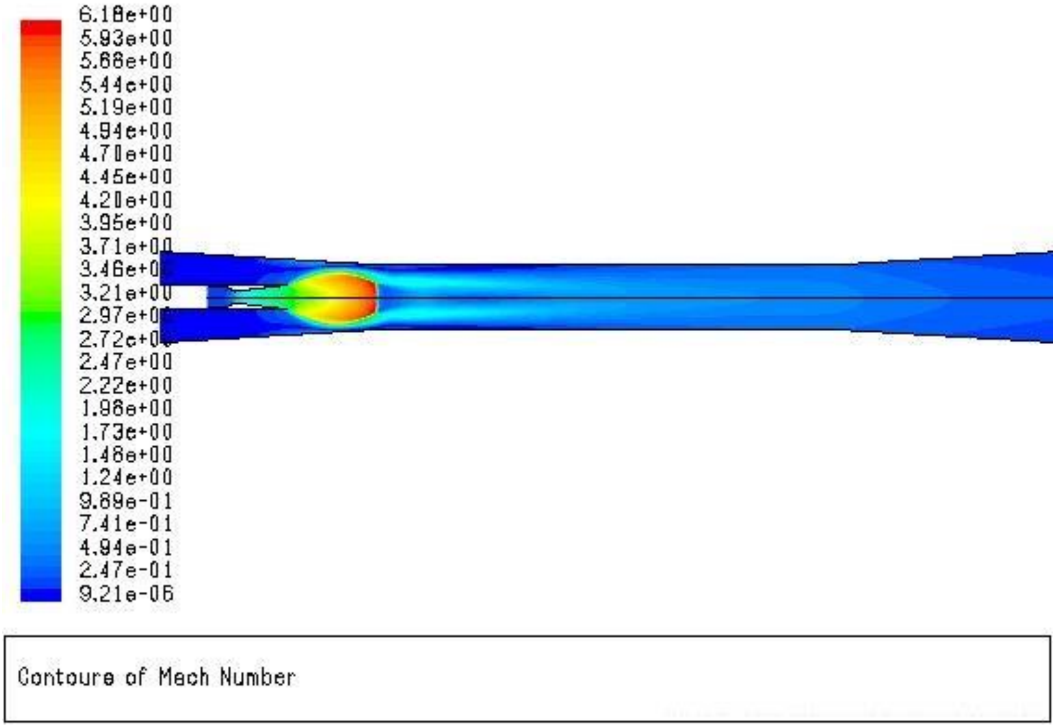

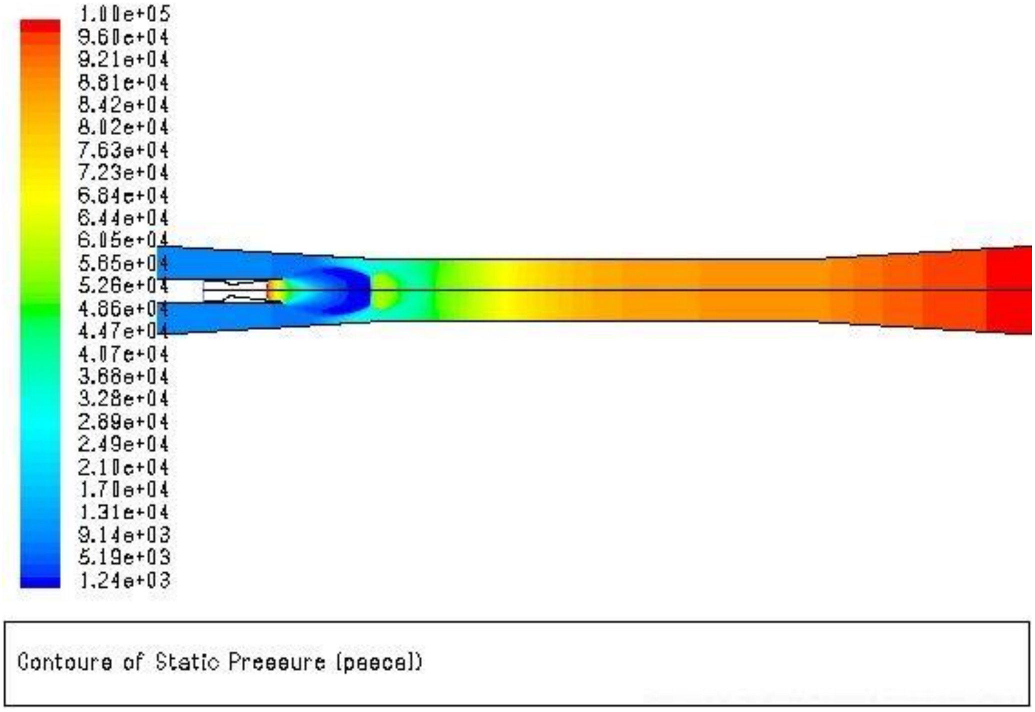

PC=25bar;MGN2=60kg/s

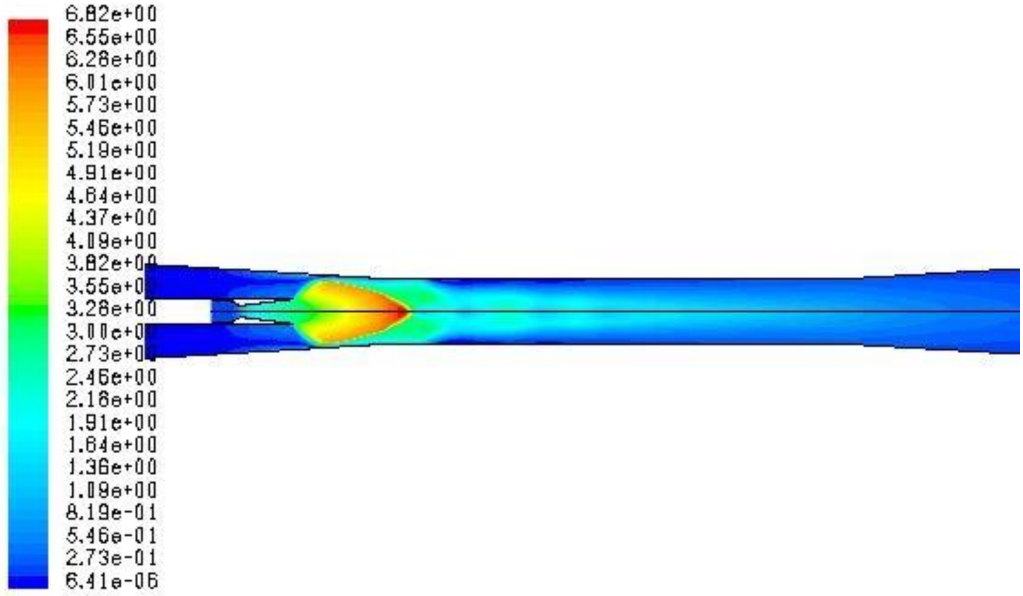

Contours of Mach Number

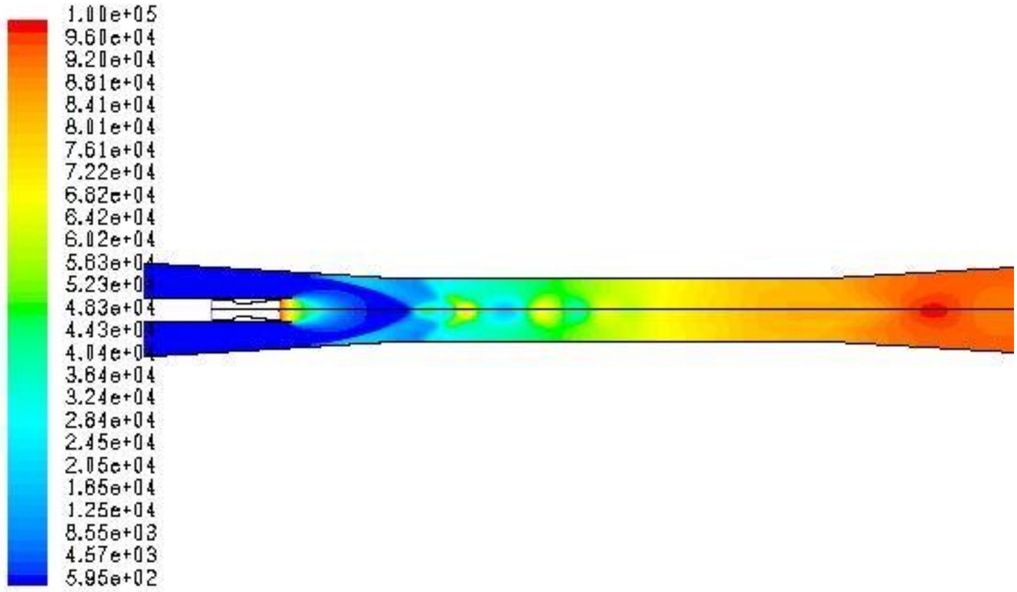

Contours of Static Pressure (pascal)

PC=30bar;MGN2=72kg/s

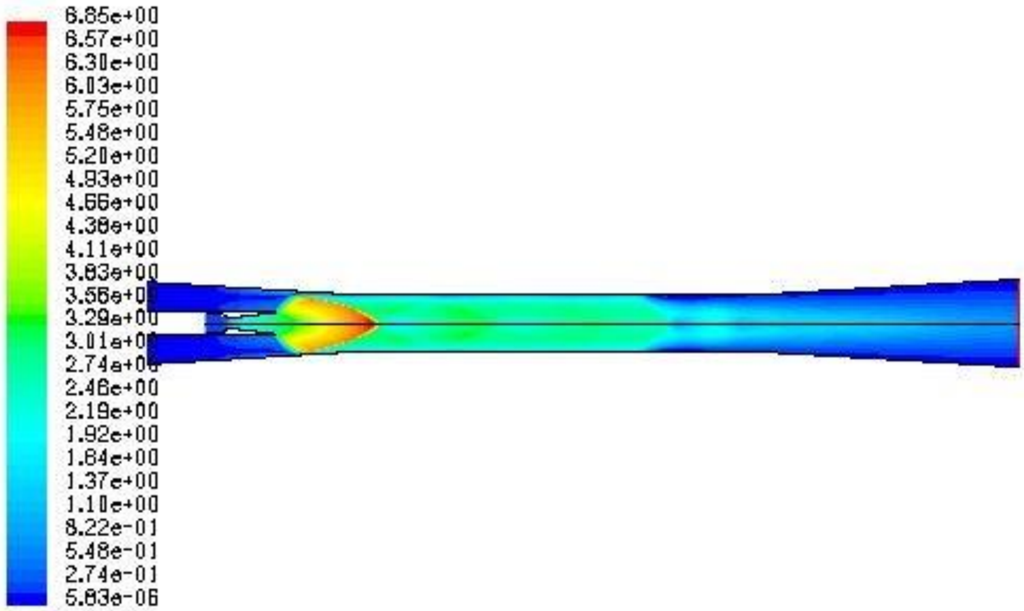

Contours of Mach Number

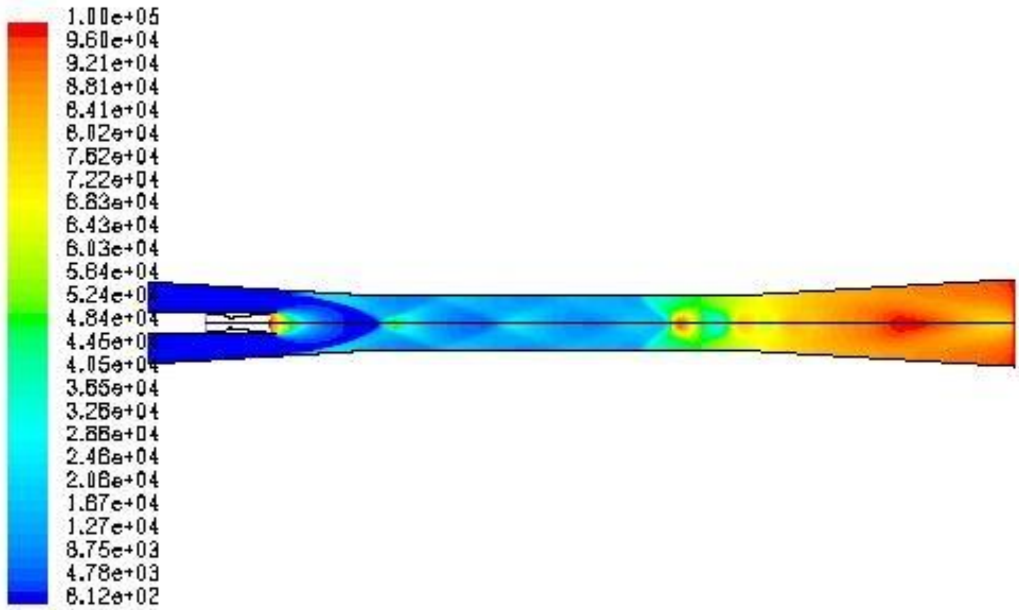

Contours of Static Pressure (pascal)

5.5 Conclusion:

Based on the above case studies, the optimum configuration of the ejector system with the nozzle A.R of 4.6, the distance between the nozzle exit and the mixer throat of 925 mm. The GN2 supply Pressure of 25 bars has arrived through detailed CFD analysis which yields the better performance of No-load suction Pr. of 22.9 m bar and the full load suction Pressure of 784.85 m bar. It is exactly matching with the one-dimensional gas dynamic equation value as well as the system requirement tor Cryo-rocket engine HAT facility.